Hartree−Fock and Density Functional Methods and IR and NMR Spectroscopies in the Examination of Tautomerism and Features of Neutral 9-Acridinamine in Gaseous and Condensed Media

Janusz Rak,[†] Piotr Skurski,[†] Maciej Gutowski,[‡] Ludwika Jóźwiak,[†] and Jerzy Błażejowski*,[†]

Departments of Chemistry, University of Gdańsk, 80-952 Gdańsk, Poland, and University of Utah, Salt Lake City, Utah 84112

Received: May 29, 1996; In Final Form: August 16, 1996[⊗]

Two tautomeric molecules, 9-acridinamine (9-AA) and 9(10*H*)-acridinimine (9-AI), were examined at the ab initio Hartree−Fock (HF) and density functional (DFT) levels of theory with the 6-31G** basis sets. Solvent (hexane, CH_3CN, H_2O) effects were included in ab initio HF optimizations through the self-consistent reaction field (SCRF) technique. Subsequent Hessian calculations followed by the normal-mode analyses revealed all harmonic frequencies to be positive, thus confirming the validity of the geometry optimizations. The energies of the molecules at stationary points corresponding to ab initio HF geometries were supplemented with the second-order Møller−Plesset (MP2) electron correlation correction. Standard routines utilizing relationships of statistical thermodynamics enabled determination of enthalpies of formation (supplemented further with corrections arising from isogyric, hydrogenation, and isodesmic processes) and entropies (heat capacities) at selected temperatures, as well as constants revealing equilibrium between two tautomeric forms. Other physicochemical characteristics, such as bond orders, dipole moments, and energies of the lowest unoccupied (LUMO) and highest occupied (HOMO) molecular orbitals were also obtained from theoretical calculations. Thermochemical data indicate that 9-AA and 9-AI should coexist at ambient temperature. This is also confirmed by a comparison of experimental IR and Raman spectra with harmonic frequencies derived theoretically. ^1H and ^{13}C chemical shifts obtained at the GIAO level of theory correlate only qualitatively with relevant experimental NMR data and do not exclude the existence of tautomeric phenomena. The distributions of atomic partial charges and electrostatic potential around the molecules differ noticeably, which implies that 9-AA and 9-AI may behave differently with respect to biomolecules.

Introduction

9-Acridinamine (the name generally used for the compound), one of the simplest representatives of the family of nitrogen organic bases, is a molecule interesting from the cognitive point of view owing to its relatively simple constitution and interesting physicochemical features, which are reflected, among other things, in its ability to interact with biomolecules.[1,2] For these reasons, 9-acridinamine has often been used as a model compound in studying the general properties of chemical entities.[3−6] Its biological relevance is exhibited by its mutagenic activity,[7−13] as well as its ability to interact with DNA[11,14−19] and other biologically important molecules.[15,20−23] Of some interest is the photodynamic activity of the compound.[24−26] 9-Acridinamine is also a convenient fluorescent probe for investigating pH and various physical features of biological systems.[27−34]

These specific features of 9-acridinamine result from the fact that the molecule contains two basic sites, one at the heterocyclic nitrogen atom and the other at the exocyclic nitrogen atom, able to participate in hydrogen bonding or electron donor−acceptor interactions. It was noted early in this century that one of the hydrogen atoms bonded to the exocyclic nitrogen atom can migrate to the endocyclic nitrogen atom, which results in the two tautomeric forms of the compound (named subsequently as 9-AA and 9-AI).[1,2,4] Despite long discussions, in which the results of investigations were interpreted in favor of the existence of 9-acridinamine in either the imino[35−38] or amino[39−44] forms, the problem still remains to be resolved. It has been the subject of some of our recent publications in which electronic absorption spectroscopy[45] and semiempirical quantum chemistry methods[4,45] were employed to demonstrate the coexistence of 9-acridinamine in the two above-mentioned tautomeric forms. This publication shows what can be said concerning the tautomerism of the compound on the higher level of theory, i.e., the ab initio Hartree−Fock and density functional methods, as well as infrared, Raman, and NMR spectroscopic investigations.

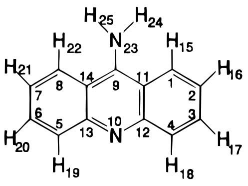

9-acridinamine (9-AA)

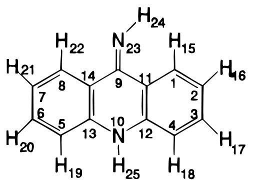

9(10H)-acridinimine (9-AI)

Methods

Quantum Mechanical Calculations. Unconstrained geometry optimizations of isolated 9-AA and 9-AI were conducted either at the Hartree−Fock (HF)[46] or the density functional (DFT)[47] levels of theory using gradient techniques[48,49] and 6-31G** basis sets.[50,51] Density functional calculations were carried out using the Becke 3LYP (B3LYP) nonlocal spin density functional approximation (which uses Becke's nonlocal exchange functional[52,53] and the Lee−Yang−Parr nonlocal correlation functional[54]). HF geometry optimizations were followed utilizing the self-consistent reaction field (SCRF)

[†] University of Gdańsk.

[‡] University of Utah.

[⊗] Abstract published in *Advance ACS Abstracts,* December 1, 1996.

S1089-5639(96)01555-1 CCC: $14.00

model,[55−57] which simulates the presence of the solvent. In the latter calculations the relative electric constants were assumed to be 2.0, 38.8, and 78.4 for hexane, acetonitrile (CH_3CN), and water (H_2O), respectively, and spherical cavity radii were evaluated as 4.78 Å for 9-AA and 4.74 Å in the case of 9-AI.[57] All HF results were finally supplemented with the second-order Møller−Plesset (MP2) electron correlation correction[58] (relevant values are referred to as MP2/6-31G**||HF/6-31G**, where "||" means "at the geometry of"). After each optimization was completed, the energy Hessian (second derivatives of the energy as a function of nuclear coordinates) was calculated and checked for positive definiteness to assess whether the structures were true minima.[46,47,59] On the basis of the numerical values of second derivatives, the harmonic vibrational frequencies were subsequently derived.[46,47,59] ^{1}H and ^{13}C magnetic shielding tensors (χ) for DFT optimized structures of 9-AA, 9-AI, and tetramethylsilane (TMS; reference) were obtained following the gauge-including atomic orbital (GIAO) approach.[60−62] The differences between isotropic magnetic shielding tensors of nuclei in TMS and 9-acridinamine ($\chi_{TMS} - \chi_{9\text{-AA(9-AI)}}$) were considered as relevant chemical shifts.[60]

All the above-mentioned calculations were conducted in the Utah Supercomputing Institute on an SGI Power Challenge 8000 server or on an HP/735 Apollo workstation using GAUSSIAN 92/DFT[63] or GAUSSIAN 94[64] program packages. Physicochemical characteristics of 9-acridinamine tautomers were extracted either directly from data files after geometry optimizations (dipole moments, energies of LUMO and HOMO) or were obtained using the routines available in GAUSSIAN (bond orders[65]). Molecular electrostatic potential around molecules was explored using the SPARTAN 4.0 program package.[66] Atomic partial charges were determined from the fit to the molecular electrostatic potential (MEP fit) at points selected according to the Besler−Merz−Kollman scheme.[67]

Thermodynamic Quantities. Energy differences between tautomeric forms (uncorrected for the zero-point vibrational energy) (ΔE) were derived to enable comparison of energetic stability of two tautomers. Values of other thermodynamic functions, namely zero-point energies (E_0), entropies (${}_TS°$), heat capacities (${}_TC_p°$), and thermal energy contributions (${}_TH° - E_0$) at a given temperature (T) and standard pressure (1 atm), were determined using the built-in GAUSSIAN statistical-mechanics routines (for this purpose theoretically determined values of harmonic vibrational frequencies and other features of molecules were used). This enabled evaluation of the energies of formation at 0 K, as well as enthalpies of formation and constants reflecting equilibrium between tautomeric forms at any temperature above 0 K.

Energies or enthalpies of formation were calculated according to Hess's Law,[68] i.e., subtracting from the energies of gaseous 9-AA or 9-AI, the energies of gaseous H_2 and N_2, and solid C (values of the latter quantity were obtained by subtracting the energy of atomization equal to 711.185 (0 K) or 716.67 (298 K, 1 atm) kJ/mol[69,70] from the energy of the gaseous entity) in the lowest electronic states, multiplied by the relevant stoichiometric coefficients, and adding the contributions of the zero-point energy ($\Delta_{f,0}E$) or additionally thermal energy at any temperature above 0 K ($\Delta_{f,T}H°$). The thermodynamic equilibrium constants (${}_TK°$) for tautomerization (t), reflecting the ratios of n(9-AI)/n(9-AA) (n − number of molecules) in the gaseous phase, were found from the relationship[68]

$$ {}_TK° = \exp[-\Delta_{t,T}G°/(RT)] \tag{1} $$

where R is the gas constant while $\Delta_{t,T}G°$ results from the Gibbs equation

$$ \Delta_{t,T}G° = \Delta_{t,T}H° - T\Delta_{t,T}S° \tag{2} $$

NMR, Vibrational Spectroscopic, and Thermogravimetric Investigations. ^{1}H and ^{13}C NMR spectra for saturated solutions of 9-acridinamine in CD_3CN were recorded on a Varian Unity 500 Plus spectrometer. 1D spectra were collected under standard conditions and chemical shifts were referred to the relevant ^{1}H or ^{13}C nuclei signals of TMS. HSQC and HMBC spectra were acquired employing the pulsed-field gradient technique.[71]

Infrared spectra of 9-acridinamine hemihydrate dispersed in KBr (4000−400 cm^{-1} region) or polyethylene (400−20 cm^{-1} region) were recorded on a Bruker IFS 66 FTIR instrument at a resolution varying between 1 and 2 cm^{-1}. Raman scattering measurements (resolution 2 cm^{-1}) were carried out on samples of the pure compound (powdered) using a Bruker FRA 106 FT-module connected to the FTIR system (an Nd^{3+}:YAG laser (1064 nm) served as excitation source).

Dynamic thermogravimetric investigations were conducted on a NETZSCH (Model TG 209) thermobalance.

Results and Discussion

Geometry and Energetics: Influence of the Environment. Both HF and DFT methods predict the almost planar skeleton of 9-AA. To some extent, the exocyclic N atom retains an amine character revealed by the pyramidal bond arrangement around it and the position (out of the acridine plane) of the two H atoms attached to it (Table 1). The $>C_{(9)}{=}N_{(23)}H_{(24)}$ fragment in 9-AI is slightly distorted from the nearly planar remainder of the molecule (which the values of the $N_{(10)}-C_{(9)}-N_{(23)}$ angle manifest). Typical aromatic bonds between the atoms forming the acridine skeleton, slightly shorter than the single $C_{(9)}-N_{(23)}$ bond in 9-AA, are predicted.[73] The bonds at the $C_{(9)}$ and $N_{(10)}$ atoms of the central ring of 9-AI are somewhat longer than those in 9-AA, whereas the $C_{(9)}-N_{(23)}$ bond has the length typical of a double bond.[73] The trend of bond order changes is inversely related to that noted for bond lengths (Table 1). HF and DFT geometries of 9-AA compare well with those revealed at the level of the semiempirical AM1 method,[4] though the $-NH_2$ group is predicted to be less planar by the former methods (contrary to the results of X-ray measurements). As has been mentioned above, HF and DFT methods predict an almost planar acridine skeleton in 9-AI, while the AM1 method revealed that the central ring is considerably folded along the $C_{(9)}\cdots N_{(10)}$ axis.[4] Inclusion of the environment in the calculations at the HF SCRF level of theory does not significantly influence the geometries of the molecules.

The possibility that 9-AA and 9-AI coexist and are thermodynamically stable depends to a first approximation on the energy difference between these tautomeric forms. According to the data presented in Table 2, 9-AI is energetically less stable than 9-AA. The positive energy difference between the imino and amino tautomers amounts to only 2.13 kJ/mol when predicted at the HF level but increases to 12.13 kJ/mol when energy calculations were supplemented with the MP2 electron correlation correction (at HF geometries). The energy difference between 9-AI and 9-AA predicted at the DFT level, amounting to 6.61 kJ/mol, may be regarded as being most reliable of the values obtained in this paper in view of recent successes of the B3LYP method in the prediction of energetics of molecules.[81] The influence of the environment at the HF SCRF level reduces the energy difference between 9-AI and 9-AA relative to that predicted for the isolated entities. On the other hand, when energy calculations included the MP2 electron correlation correction (at HF SCRF geometries), the energy gap between

TABLE 1: Geometric Parameters (Bond Length in Å, Angles in deg)

			bond length		bond order[a]		valence angle	dihedral angle	
state/medium	method	cpd	$C_{(9)}N_{(23)}$	$N_{(10)}C_{(12)}$	$C_{(9)}N_{(23)}$	$N_{(10)}C_{(12)}$	$N_{(10)}C_{(9)}N_{(23)}$	$C_{(12)}N_{(10)}$ $C_{(13)}C_{(14)}$	$C_{(11)}C_{(9)}$ $N_{(23)}H_{(24)}$
gaseous	HF/6-31G**	9-AA	1.375	1.324	0.333	0.485	179.1	1.15	22.93
		9-AI	1.263	1.373	0.675	0.248	176.0	0.00	0.00
	DFT/6-31G**	9-AA	1.402	1.344	0.331	0.475	179.0	1.39	24.99
		9-AI	1.289	1.380	0.660	0.240	175.7	0.00	0.00
liquid/hexane	HF/6-31G**	9-AA	1.372	1.325	0.271	0.363	179.2	1.07	22.31
		9-AI	1.264	1.373	0.549	0.178	176.0	0.03	0.00
liquid/CH_3CN	HF/6-31G**	9-AA	1.367	1.325	0.271	0.363	179.4	0.93	20.67
		9-AI	1.265	1.373	0.548	0.178	176.1	0.00	−0.02
liquid/H_2O	HF/6-31G**	9-AA	1.367	1.325	0.271	0.363	179.4	0.93	20.60
		9-AI	1.265	1.373	0.548	0.178	176.1	0.00	0.00
solid[b]	X-ray	9-AA	1.354	1.351			179.3	1.4	8.6

[a] Originating from Mulliken population analysis.[65] [b] Reference 72.

TABLE 2: Thermodynamic Data Characterizing 9-AA and 9-AI, and Equilibrium between (9-AA ⇌ 9-AI)[a]

			$\Delta_{f,0}E$		$\Delta_{f,298}H°$ [b]		$_{298}S°$		$_{298}C_p°$		
state/medium	energy||geometry	ΔE	9-AA	9-AI	9-AA	9-AI	9-AA	9-AI	9-AA	9-AI	$_{298}K°$
gaseous	HF/6-31G**||HF/6-31G**	2.13	2838.3	2841.3	2772.3	2775.1	411.2	418.6	184.4	181.3	0.787
			618.6[c]	621.5[c]	670.2[c]	673.0[c]					
					711.9[d]	714.7[d]					
					146.9[e]	154.3[e]					
	MP2/6-31G**||HF/6-31G**	12.13	490.2	503.2	424.2	437.0					0.0139
			−278.4[c]	−265.4[c]	−224.7[c]	−211.9[c]					
					325.7[d]	338.5[d]					
					401.8[e]	411.2[e]					
	DFT/6-31G**||DFT/6-31G**	6.61	364.1	371.1	299.9	306.8	421.8	426.4	199.0	196.6	0.107
			542.6[c]	549.6[c]	598.1[c]	605.0[c]					
					441.3[d]	448.2[d]					
					128.0[e]	138.3[e]					
liquid/hexane	HF/6-31G**||HF/6-31G**	1.82									
	MP2/6-31G**||HF/6-31G**	11.60									
liquid/CH_3CN	HF/6-31G**||HF/6-31G**	1.21									
	MP2/6-31G**||HF/6-31G**	16.43									
liquid/H_2O	HF/6-31G**||HF/6-31G**	1.18									
	MP2/6-31G**||HF/6-31G**	16.61									

[a] $\Delta E = E_{9\text{-AI}} - E_{9\text{-AA}}$ (in kJ/mol). $\Delta_{f,0}E$ and $\Delta_{f,298}H°$ (in kJ/mol) represent the energy (0 K) and enthalpy (298 K) of formation, respectively. $_{298}S°$ and $_{298}C_p°$ (in J/(mol K)) denote the entropy and heat capacity, respectively, and $_{298}K°$ is the thermodynamic equilibrium constant. [b] The experimental value of the enthalpy of formation of gaseous 9-acridinamine ($\Delta_{f,298}H°$ equal to 273 kJ/mol) was estimated by taking the enthalpy of formation of the crystalline compound from ref 74 (equal to 159.0 kJ/mol) and adding the enthalpy of sublimation ($\Delta_s H°$) determined by approximating thermogravimetric curves (recorded in this work) with the Clausius−Clapeyron equation[68] (as described in ref 75). $\Delta_s H° = 114$ kJ/mol. [c] Values supplemented with the isogyric correction (an isogyric precess is one, in which the number of unpaired electron spins is left unchanged[76]) amounting to 21 times the difference between the experimental (equal to −432.1 kJ/mol at 0 K and −436.0 kJ/mol at 298 K[69,70]) and relevant theoretical values of the enthalpy of reaction $H + H \rightarrow H_2$[76,77] (values represent total corrections corresponding to 0 and 298 K (in kJ/mol), respectively: −2219.7 and −2102.1 (HF), −768.6 and −648.9 (MP2), 178.5 and 298.2 (DFT)). [d] Values supplemented with the correction arising from the consideration of the hydrogenation reaction (2-AA or 2-AI + $24H_2 \rightarrow 13CH_4 + 2NH_3$, the number of chemical bonds in such a process remains unchanged[77]), which amounts to 13 times the difference between the experimental (−74.4 kJ/mol[70,78]) and theoretical value of the enthalpy of formation of CH_4 plus twice the difference between experimental (−45.9 kJ/mol[70]) and theoretical value of the enthalpy of formation of NH_3 (this correction at 298 K equals (in kJ/mol): −2060.4 (HF), −98.5 (MP2), and 141.4 (DFT)). [e] Values supplemented with the corrections arising from the consideration of isodesmic reactions[79,80] 2-AA + $24H_3CCH_3 \rightarrow 8HC(CH_3)_3 + 5C(CH_3)_4 + H_2NCH_3 + N(CH_3)_3$ or 2-AI + $24H_3CCH_3 \rightarrow 8HC(CH_3)_3 + 5C(CH_3)_4 + 2HN(CH_3)_2$ (these processes conserve the number and the nature of chemical bonds[77]), which are equal to the sum of the differences between the experimental ($\Delta_{f,298}H°$ equal to (in kJ/mol): −83.8, −134.2, −168.1, −22.7, −18.5, and −23.7 for H_3CCH_3, $HC(CH_3)_3$, $C(CH_3)_4$, H_2NCH_3, $HN(CH_3)_2$, and $N(CH_3)_3$, respectively[70,78]) and theoretical value of the enthalpy of formation of all reactants (with the exception of the molecule studied) multiplied by the relevant stoichiometric coefficients (negative in the case of H_3CCH_3) (these corrections at 298 K equal (in kJ/mol): −2625.4 for 9-AA and −2620.8 for 9-AI (HF), −22.4 for 9-AA and −25.8 for 9-AI (MP2), −171.9 for 9-AA and −168.5 for 9-AI (DFT)).

9-AI and 9-AA was even higher than for the isolated species. The conclusion that arises upon examining the energy characteristics compiled in Table 2 is that the inclusion of solvation effects does not substantially influence the energy difference between 9-AI and 9-AA, and since this difference is relatively small, one may expect both tautomeric forms to coexist in the gaseous and liquid phases.

Thermochemistry: Influence of Temperature on Tautomeric Equilibria. To gain an insight as to how far theoretically predicted values of thermochemical quantities conform with the experimental ones, the energies of formation of 9-AA and 9-AI at 0 K and standard enthalpies of formation of both gaseous entities at 298 K arising from the theory were compared in Table 2 with the standard enthalpy of formation of 9-acridinamine originating from the experiment. Discrepancies are the most pronounced when the experimental value of the enthalpy of formation is compared with the theoretical one relevant to the HF level of theory. Closer to the experimental value of $\Delta_{f,298}H°$ are those obtained at the DFT or, as a result of inclusion of the electron correlation correction, at the MP2 level. Hoping to obtain better conformity between both types of thermochemical characteristics, we supplemented the theoretical enthalpies of

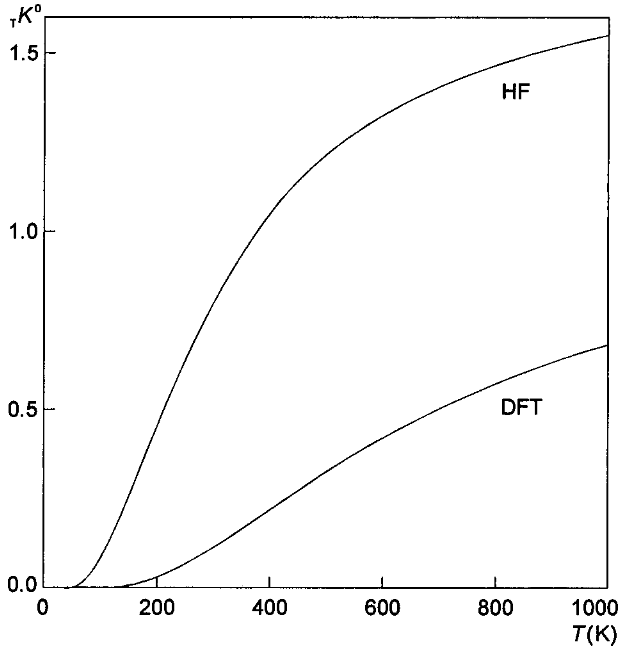

Figure 1. Thermodynamic equilibrium constant $_TK°$ (ratio of the number of 9-AI to 9-AA in the gaseous phase) versus temperature (T).

formation with corrections arising from a consideration of isogyric,[76,77] hydrogenation,[77] or isodesmic[77,79,80] reactions (relevant values are given in Table 2). In fact, data relevant to the DFT level not supplemented with any correction fit the experimental value best. This finding seems to support the opinion that the DFT (B3LYP) approach is very useful in studying the thermodynamics of chemical systems.[81]

The $\Delta_{f,298}H°$ gaps always match ΔE closely despite the substantial discrepancies between the theoretical enthalpies of formation and the experimental one, which led us to believe that the deficiencies of the theoretical approaches vanish when the thermodynamics of tautomeric equilibria is considered. Thus, by combination of the values of the enthalpy and entropy differences between 9-AI and 9-AA, the equilibrium constants at the standard pressure and ambient temperature were derived (Table 2). The value of $_{298}K°$ arising from the HF calculations shows that the molar ratio of 9-AI/9-AA would be 0.79, while that originating from the DFT method would be only 0.11. Inclusion of the MP2 electron correlation correction in the energy term decreases this ratio to 0.01 (this latter result is, however, less certain, since energy and geometry do not correspond to the same level of theory[82]).

The equilibrium between the tautomeric forms in the gaseous phase is affected by the temperature as demonstrated in Figure 1. At 0 K, where equilibrium is affected exclusively by the energy factor, only the lowest energy form (9-AA) would occur. When the temperature increases, the thermodynamic equilibrium constant gradually increases, which means that the number of 9-AI molecules rises relative to that of 9-AA molecules. The tendency of $_TK°$ changes is similar for data originating from HF and DFT calculations; however, numerical values are strongly influenced by the energy difference between 9-AI and 9-AA, which is lower in the former case.

Since it is not possible to assess thermal energy (energy above 0 K related to heat capacity at a given temperature; heat capacities at ambient temperature are given in Table 2) and entropy contributions in liquid phases (classical statistical mechanics do not apply to such cases), it is also impossible to evaluate, to a reliable degree of certainty, the influence of the environment on values of thermodynamic quantities and equilibrium constants. Nevertheless, taking into account similarities in the constitution of 9-AA and 9-AI, one may suppose that thermal energy and entropy are similarly influenced by solvation, which led to the belief that both the above tautomeric forms could be present in liquid phases.

The data in Figure 1 show that within relatively narrow temperature limits, relevant to the existence of a given phase (e.g., 273−373 K in the case of water), equilibrium constants differ only by a small percentage. If the dependencies obtained for the gaseous phase held for liquid phases, one would not expect substantial changes in the ratios of possible tautomers in the latter phases, following temperature changes.

Physicochemical Characteristics. According to Koopmans' theorem[83] (which does not apply to the density functional formalism[84]), the negative energies of the lowest unoccupied (LUMO) and highest occupied (HOMO) molecular orbitals (Table 3) approximate the electron affinity (EA) and the first ionization potential (IP) of a molecule, respectively.[85,86] HF energies of LUMO, always positive and somewhat higher in the case of 9-AI, suggest that an electron attachment would lead to unstable negative ions of both tautomers. HF energies of HOMO indicate that the ionization of 9-AA should proceed more easily than that of 9-AI. This causes the LUMO−HOMO energy gap to be ca. 0.8 eV higher in the case of 9-AI than 9-AA and suggests a somewhat higher stability of the former entity.[87] Inclusion of the environment has only a minor effect on the values of these two characteristics.

The dipole moments predicted for the isolated molecules at the HF and DFT levels are somewhat higher in the case of 9-AI (Table 3). The application of the AM1 method revealed the reverse tendency.[4] Inclusion of the environment in the HF calculations results in dipole moments becoming higher than those of isolated entities and increasing with the increase in the polarity of the medium. The experimentally obtained value of the dipole moment of 9-acridinamine in benzene, equal to 4.14 D,[39,40] lies between those predicted for 9-AA and 9-AI in hexane (3.95 and 4.28 D, respectively), which could indicate that the former value results from the coexistence of the two tautomeric forms of 9-acridinamine in the liquid phase.

TABLE 3: Physicochemical Properties of 9-Acridinamine and 9(10*H*)-Acridinimine

			energy (eV)			atomic partial charges				
state/medium	method	compound	LUMO	HOMO	dipole moment (D)	C(9)	N(10)	N(23)	H(24)	H(25)
gaseous	HF	9-AA	1.865	−7.165	3.59	0.454	−0.799	−0.862	0.376	0.377
		9-AI	2.428	−7.396	3.87	0.706	−0.743	−0.880	0.383	0.401
	DFT	9-AA			3.41	0.422	−0.776	−0.857	0.369	0.372
		9-AI			3.84	0.656	−0.732	−0.858	0.371	0.399
liquid/hexane	HF	9-AA	1.872	−7.153	3.95	0.458	−0.806	−0.866	0.381	0.382
		9-AI	2.420	−7.396	4.28	0.714	−0.744	−0.889	0.383	0.403
liquid/CH_3CN	HF	9-AA	1.889	−7.127	4.64	0.465	−0.817	−0.871	0.390	0.390
		9-AI	2.404	−7.397	5.05	0.728	−0.746	−0.906	0.382	0.407
liquid/H_2O	HF	9-AA	1.889	−7.126	4.66	0.465	−0.818	−0.871	0.390	0.390
		9-AI	2.403	−7.396	5.09	0.729	−0.747	−0.906	0.382	0.408

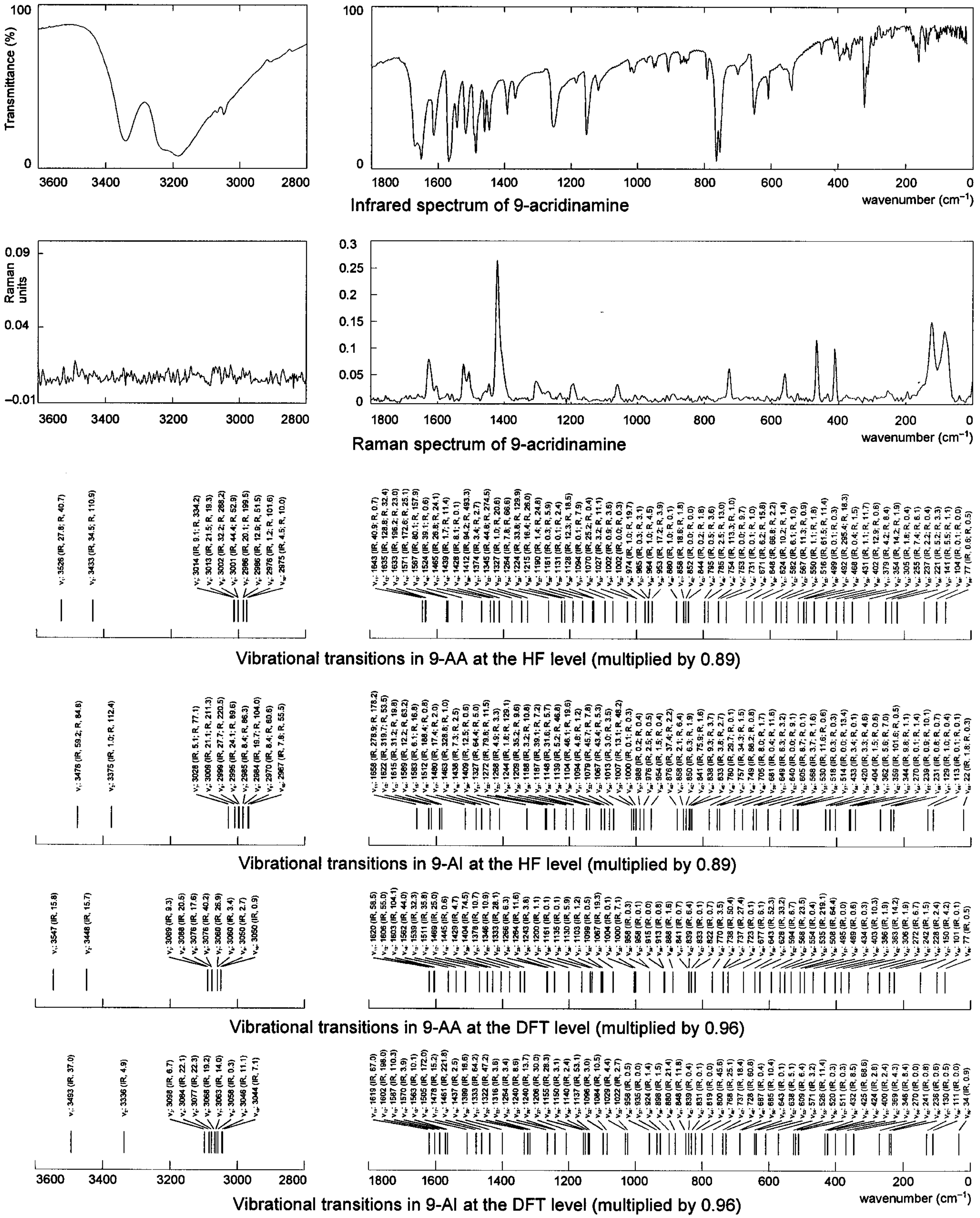

Figure 2. Infrared (IR) and Raman (R) spectra of 9-acridinamine together with the theoretically predicted vibrational transitions in 9-AA and 9-AI (numbers following "IR" and "R" in parentheses indicate infrared intensities in KM/mol and Raman scattering activities in Å^4/amu, respectively).

The dipole moment reflects the nonuniform distribution of a charge and thus the electrostatic potential around molecules. Two zones of the potential centered at nitrogen atoms appear in the molecules. The negative potential region is in the neighborhood of the endocyclic nitrogen of 9-AA and the exocyclic nitrogen of 9-AI, while the zone of positive potential occurs at the exocyclic nitrogen of 9-AA and the endocyclic nitrogen of 9-AI. This feature is reflected in the atomic partial charges, derived so as to reproduce the molecular electrostatic potential, shown for selected atoms in Table 3. An excess negative charge is predicted at endocyclic and a somewhat higher one at exocyclic nitrogen atoms. The negative charge is always higher at the endocyclic N atom in 9-AA and at the exocyclic N atom in 9-AI, which results in the negative charge

TABLE 4: Harmonic Frequencies (cm^{-1}) of Selected Vibrational Modes Involving Nitrogen Atoms of 9-AA and 9-AI Calculated at the HF or DFT Level Together with Relevant Experimental Data

mode		frequency					
		theoretical		scaled[c]		obsd	
assignment	description	HF[a]	DFT[b]	HF	DFT	IR	Raman
		9-AA					
$\nu_{62}(a'')$	as $C_{(9)}N_{(23)}$ bending; $N_{(23)}H_2$ torsion	398 (4.2; 1.9)	378 (14.2)	354	363	365	
$\nu_{60}(a')$	s $N_{(23)}H_2$ deformation; ring deformation	451 (12.9; 0.6)	420 (10.3)	402	403	396	397
$\nu_{54}(a'')$	as $N_{(23)}H_2$ wagging; ring deformation	618 (1.1; 1.8)	577 (0.4)	550	554	538	541
$\nu_{40}(a'')$	as $C_{(9)}N_{(23)}$ bending; ring deformation	988 (1.0; 0.1)	925 (1.5)	880	888	870	
$\nu_{29}(a'')$	as $N_{(23)}H_2$ bending; CH bending	1271 (0.1; 2.4)	1183 (0.1)	1131	1135	1119	
$\nu_{15}(a')$	s $N_{(23)}H_2$ scissors; ring bond stretching	1761 (80.1; 157.9)	1603 (32.3)	1567	1539	1568	1568
$\nu_{14}(a'')$	as $C_{(9)}N_{(23)}$ bending; $N_{(23)}H_2$ bending; ring bond stretching	1765 (172.6; 25.1)	1627 (44.0)	1571	1562	1568	1568
$\nu_{13}(a')$	s $N_{(23)}H_2$ scissors	1834 (196.2; 23.0)	1670 (104.1)	1633	1603	1651	
$\nu_{11}(a')$	s $N_{(23)}H_2$ scissors; ring bond stretching	1846 (40.9; 0.7)	1688 (58.5)	1643	1620		
$\nu_{2}(a')$	s $N_{(23)}H$ stretching[d]	3857 (34.5; 110.9)	3591 (15.7)	3433	3448		
$\nu_{1}(a'')$	as $N_{(23)}H$ stretching[d]	3962 (27.8; 40.7)	3694 (15.8)	3526	3547		
		9-AI					
$\nu_{62}(a)$	$N_{(10)}H_{(25)}$ bending	403 (101.6; 0.5)	385 (4.3)	359	369	365	
$\nu_{28}(a)$	$N_{(23)}H_{(24)}$ and CH bending	1289 (31.6; 5.7)	1203 (28.3)	1148	1155	1156	1151
$\nu_{21}(a)$	$N_{(23)}H_{(24)}$ bending; ring deformation	1492 (64.4; 5.0)	1388 (64.2)	1327	1333		
$\nu_{15}(a)$	$N_{(10)}H_{(25)}$ bending;	1778 (6.1; 16.8)		1583		1568	1568
$\nu_{14}(a)$	ring deformation		1635 (3.9)		1570	1568	1568
$\nu_{12}(a)$	$N_{(10)}H_{(25)}$ bending; ring deformation	1822 (319.7; 53.5)	1669 (198.0)	1622	1602	1613	
$\nu_{11}(a)$	$N_{(23)}H_{(24)}$ bending; ring deformation	1863 (278.9; 178.2)	1686 (67.0)	1658	1619	1669	
$\nu_{2}(a)$	$N_{(23)}H_{(24)}$ stretching	3792 (1.0; 112.4)	3474 (4.9)	3375	3336	3343	
$\nu_{1}(a)$	$N_{(10)}H_{(25)}$ stretching	3905 (59.2; 84.8)	3638 (37.0)	3476	3493		

[a] IR intensities (KM/mol; first value) and Raman scattering activities (Å^4/amu; second value) are given in parentheses. [b] IR intensities (KM/mol) are given in parentheses. [c] Values obtained by multiplying theoretical frequencies by 0.89 (HF) or 0.96 (DFT). [d] Two NH bonds of NH_2 are involved in the stretching mode.

difference in its imino tautomer being more pronounced. A negative charge deficiency is predicted at the $C_{(9)}$ atom (much higher in 9-AI), whereas at other C atoms an excess of negative charge is expected. Finally, a negative charge deficiency is always present at the hydrogen atoms. These findings led to the belief that transfer of the hydrogen atom, following the structural change from amino to imino, is accompanied by the migration of an electric pole in the opposite direction and thus inversion in the direction of the dipole moment (which we noted earlier[4]). Nitrogen atoms may primarily be considered as sites of specific interactions, including solute−solvent interactions and those leading to the formation of associates or complexes with biomolecules.[4,88] It is thus possible that 9-acridinamine tautomers behave differently in the presence of macromolecules in living matter.

Vibrational Spectra versus Theoretical Harmonic Transitions. Infrared and Raman spectra of 9-acridinamine together with theoretically determined vibrational frequencies (scaled) are presented in Figure 2. Certain deformations of molecules as a whole or their fragments correspond to each of 69 normal modes predicted theoretically at the HF or DFT level, shown in the lower part of Figure 2. Since a complete description of all vibrational modes would require considerable space, we compiled in Table 4 only selected ones in which nitrogen atoms are involved. With several exceptions, molecular deformations match each other for modes of the same number determined on the HF and DFT levels. This forms a reliable basis for ascribing theoretically predicted frequencies of vibrational transitions to those extracted from the experimental IR and/or Raman spectra. Rough comparison of both types of characteristics reveals that theoretical frequencies appear at higher wavenumbers than peaks in experimental spectra. Thus, wavenumbers of selected strong transitions determined at the HF level were initially scaled down by the 0.89 factor recommended in the literature[46,57] and ascribed to peaks in experimental spectra of 9-AA and/or 9-AI. Subsequently, the most appropriate theoretical transitions were ascribed to the remaining peaks in the experimental spectra. The procedure was repeated until all peaks in the experimental spectra were related to one or sometimes more than one theoretical vibrational modes of 9-AA or 9-AI. The scaling factor was then derived and the mean value of 0.89 confirmed. DFT wavenumbers match experimental spectra much better than HF results, a fact confirmed in other studies.[81,89] Nonetheless, most theoretical frequencies are systematically shifted toward values higher than the experimental ones. Thus, following the procedure described above, we ascribed DFT wavenumbers to peaks in experimental IR and/or Raman spectra. The best match of characteristics of both types was obtained for a scaling factor of 0.96.

The above analysis presents an interesting example of the application of the theory to an examination of experimental vibrational spectra. Nevertheless, our primary aim was to find whether any indications as to the coexistence of 9-acridinamine in two tautomeric forms could be found on this basis. Thus,

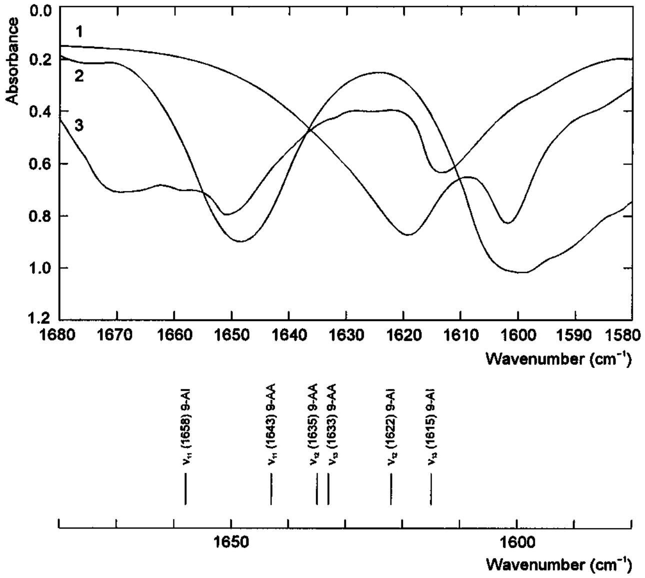

Figure 3. Infrared spectra of benzenamine (1), 4-pyridinamine (2), and 9-acridinamine (3) in the 1580−1680 cm^{-1} region together with wavenumbers (scaled) of ν_{11}, ν_{12}, and ν_{13} vibrational modes of 9-AA and 9-AI (relevant to HF level of theory).

we examined vibrational transitions throughout the whole range of experimental and/or theoretical wavenumbers with the intention of finding those characteristic of only one of the tautomeric forms. As Figure 2 demonstrates, the appropriate spectral regions for such an analysis are primarily those in which vibrations involving the nitrogen atoms appear, i.e., listed in Table 4. Careful comparison indicates that one of the most characteristic is the region between 1580 and 1680 cm^{-1} in which $-NH_2$(9-AA) and $>N-H$(9-AI) bending vibrations fall. The three peaks in the IR spectrum of 9-acridinamine can be ascribed to the following: ν_{12}(a) $N_{(10)}H_{(25)}$ bending mode and ν_{13}(a) ring deformation mode of 9-AI (1613 cm^{-1}); $\nu_{11}(a')$ symmetric $N_{(23)}H_{(24)}H_{25}$ bending mode, $\nu_{12}(a'')$ asymmetric ring deformation mode, and $\nu_{13}(a')$ symmetric $N_{(23)}H_{(24)}H_{(25)}$ bending mode of 9-AA (1651 cm^{-1}); ν_{11}(a) $N_{23}H_{24}$ bending mode of 9-AI (1669 cm^{-1}). To provide more evidence confirming the validity of such an assignment in Figure 3, we plotted IR absorption spectra of 9-acridinamine, 4-pyridinamine (the simplest molecule containing endocyclic and exocyclic N atoms situated exactly as in 9-acridinamine; the respective energy differences of the imino and amino tautomers of 4-pyridinamine predicted at the HF/6-31G** and DFT(B3LYP)/6-31G** level of theory are equal to 83.2 and 74.8 kJ/mol, which implies that the amino tautomer should be predominant), and benzenamine (the simplest aromatic amine). As can be noted, the IR spectra of benzenamine and 4-pyridinamine exhibit only two peaks in the 1580−1680 cm^{-1} region (one pair match at 1602 cm^{-1}), while 9-acridinamine displays three peaks (one of them (1651 cm^{-1}) matches one of the two 4-pyridinamine peaks (1649 cm^{-1})). Furthermore, the peak in 9-acridinamine at 1669 cm^{-1} appears in the region where neither 4-pyridinamine nor benzenamine exhibits any absorption. This peak might therefore have originated from the imino form of 9-acridinamine.

Examining the whole spectral region (Figure 2), one can find peaks that correspond to theoretical transitions in either 9-AA or 9-AI and sometimes equally well to those in both tautomers.

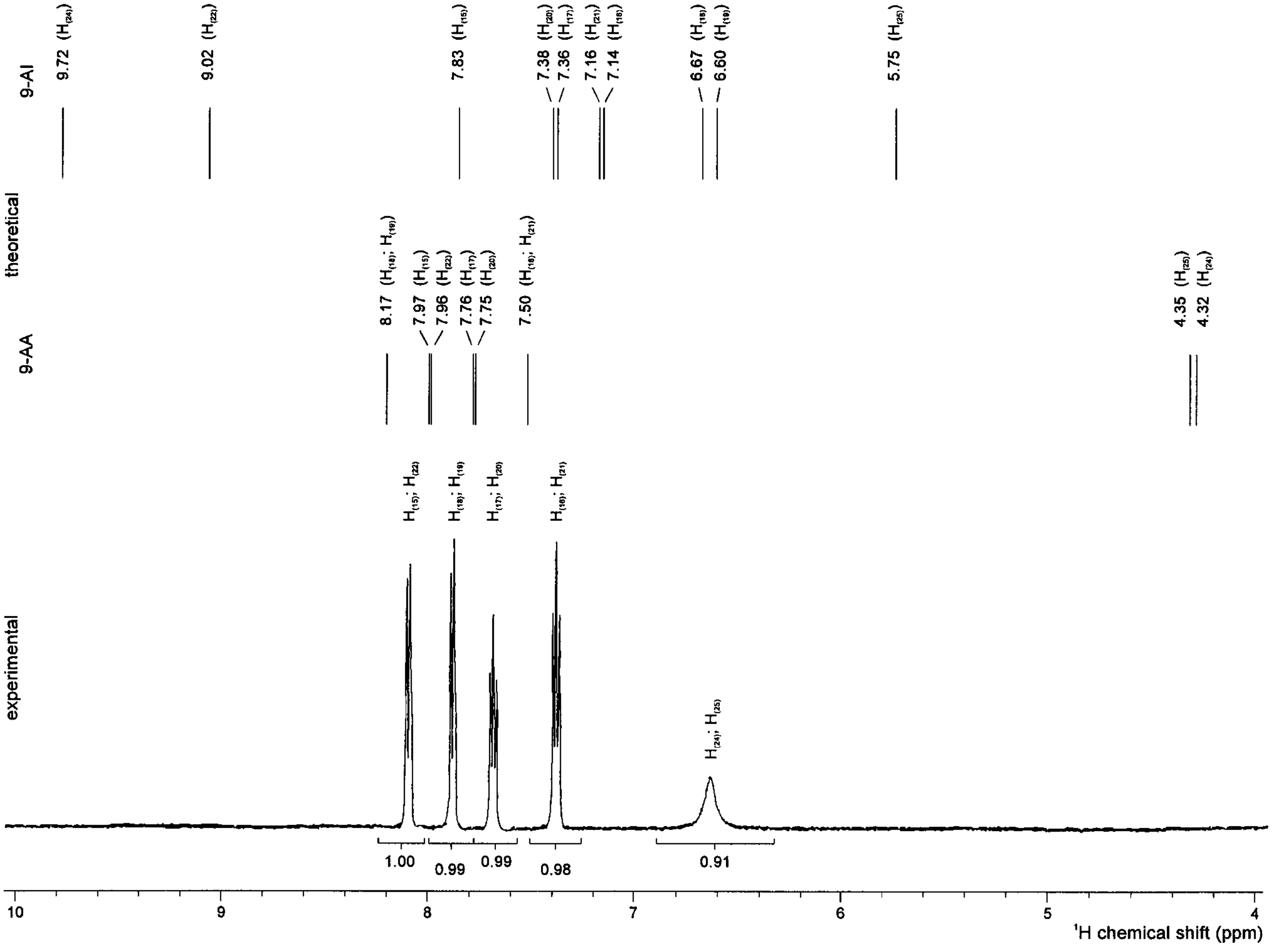

Figure 4. ¹H NMR spectrum of 9-acridinamine dissolved in CD_3CN (recorded at 228 K) together with chemical shifts predicted by the GIAO method.

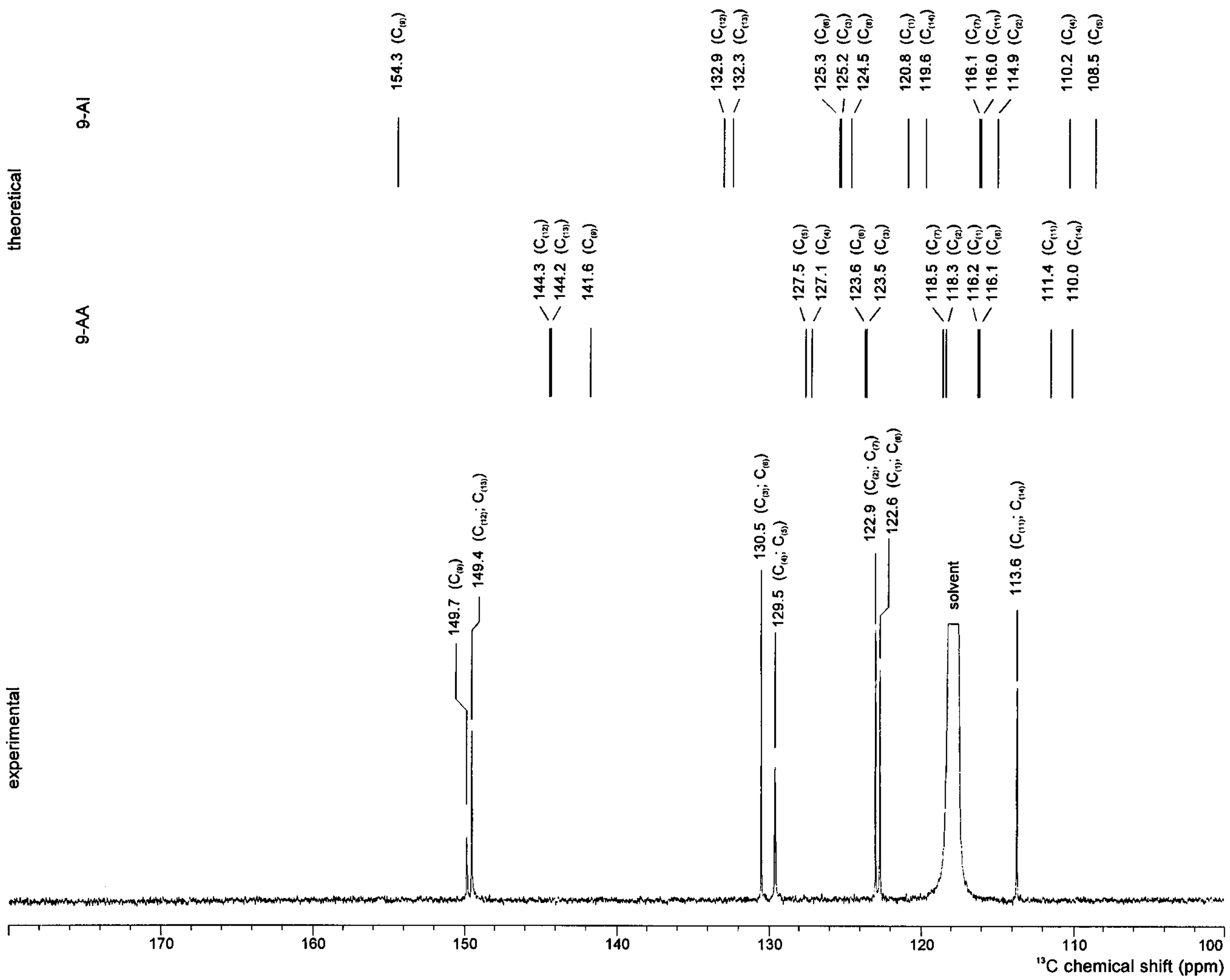

Figure 5. ^{13}C NMR spectrum of 9-acridinamine dissolved in CD_3CN (recorded at 298 K) together with chemical shifts predicted by the GIAO method.

Therefore, vibrational spectroscopic analysis provides some evidence of the coexistence of the two tautomeric forms of 9-acridinamine in condensed phases. Several earlier IR spectroscopic studies led to similar conclusions,[36,42,90,91] although others did not.[39,92]

It is perhaps worth mentioning that although the 9-AA tautomer was originally used for the preparation of pellets (hemihydrate[72]), it may convert to the 9-AI form under pressure (examples of pressure-induced tautomerization are known, e.g., in 3-acridinol[93]).

NMR Spectra versus Theoretical Chemical Shifts. The ^{1}H NMR spectrum of 9-acridinamine consists of a system of four signals arising from the eight aromatic hydrogen atoms and a broad signal originating from the two hydrogen atoms attached to the nitrogen atom(s) (Figure 4). The ^{13}C NMR spectrum of the compound displays seven clearly visible signals (Figure 5). Since it was not possible on the basis of these spectra to assign signals to particular atoms,[94] we used HSQC and HMBC (2D spectra are not presented here), as well as decoupling techniques for this purpose.[71] The assignments are given in Figures 4 and 5, where at all signals the relevant atoms from which they originate are indicated. This assignment was tentatively completed assuming the 9-AA structure of the compound and following, whenever possible, the results of the GIAO method. It was based on two premises. First, chemical shifts of the aromatic H atoms of 9-AA predicted theoretically fall in the region of experimental signals and the pattern, as well as the mutual arrangement of both types of characteristics, is similar. Moreover, the ^{1}H NMR spectrum of *N*,*N*-dimethyl-9-acridinamine (not published here), i.e., the compound with a blocked amino structure, is very similar to that of 9-acridinamine. As can be seen, the ^{13}C chemical shifts predicted by the GIAO method for 9-AA do not correlate with the experimental ones for 9-acridinamine either with respect to numerical values or the mutual relations. On the other hand, theoretical and experimental ^{1}H chemical shifts differ by no more than a few percent and the alternation of signals is, with one exception, the same in both spectra.

Our assignment of ^{13}C signals fits excellently those reported in refs 95 and 96 but differs from that in ref 97. As far as ^{1}H signals are concerned, our assignment differs from those reported in refs 43 and 97. Since our data were obtained by advanced techniques, they represent the true chemical shifts of ^{1}H and ^{13}C nuclei in 9-acridinamine.

The ^{1}H NMR signal relevant to the two H atoms attached to the N atom(s) in the experimental spectrum is broad (broadening enhances with an increase of temperature), and its chemical shift is noticeably higher than that predicted by the GIAO method for the H atoms of the $-NH_2$ group in 9-AA, even though it is located between those of the H atoms of the $>N-H$ fragments in 9-AI. The $-NH_2$ group usually gives only one signal in the ^{1}H NMR spectra.[43] On the other hand, the broad signal in the ^{1}H NMR spectrum of 9-acridinamine (Figure 4) might well originate from the hydrogen atoms being exchanged with other molecules.[71,93] Such an exchange could take place between two tautomeric forms of 9-acridinamine (i.e., 9-AA or 9-AI molecules) or with the participation of water (solvent) molecules (traces of water are present in the solution, since 9-acridinamine crystallizes as a hemihydrate[72]). The occurrence of these processes could cause the tautomeric equilibrium between 9-AA and 9-AI to be achieved in the CD_3CN liquid phase (as the theoretical predictions on the HF level indicate). In such a case signals in the experimental NMR spectra could arise from a metastable transition state formed upon rapid exchange of two H atoms between two 9-AA or 9-AI molecules, or one H atom through a bridge of water (solvent) molecules spread between the N atoms of one 9-acridinamine molecule.[98] In such a state the signals could be the resultant of those originating from both 9-AA and 9-AI. Indeed, examination of the ^1H and ^{13}C chemical shifts of the two theoretically predicted tautomeric forms reveals that both these characteristics fall in the region where signals in experimental spectra appear, and their superposition could give a result similar to the experimental one. This could also explain why we were unable to observe the deuterium isotope effects on ^{13}C nuclear shielding.[93] In summary, NMR studies do not exclude tautomeric phenomena in 9-acridinamine.

The results of earlier NMR investigations tended to be interpreted in favor of the amino form of 9-acridinamine.[43,95,96]

Tautomerism of 9-Acridinamine in View of Theoretical and Experimental Findings. The theoretically determined difference in energy between 9-AI and 9-AA is always positive, which means that the amino tautomer is energetically more stable. The entropy difference, however, is positive, which implies that from the thermodynamic probability point of view the imino tautomer should be the more stable form, at least in the gaseous phase. The free enthalpy (energy) difference, combining the two above-mentioned effects, is the most positive at 0 K but becomes less positive or even negative with an increase in temperature. This means that at elevated temperatures the imino tautomer becomes thermodynamically favored. The free enthalpy difference amounts to 0, which corresponds to the state in which the ratio of the number of 9-AI/9-AA equals 1, at 371 or 2052 K, depending on whether the data are derived from HF or DFT methods. The above discussion indicates that at least in the gaseous phase, the coexistence of both 9-acridinamine tautomers should be expected at ambient and elevated temperatures. Confirmation of this finding would be possible if one could concentrate a suitable number of molecules in the gaseous phase. Unfortunately, the vapor pressure of 9-acridinamine is very low up to 400 K (evaluated on the basis of thermogravimetric data, the sublimation temperature is 534 K at atmospheric pressure, and the vapor pressures at 298 and 398 K are equal to 1.5×10^{-9} and 1.5×10^{-4} atm, respectively). This makes investigations in the gaseous state difficult. We therefore turned our attention to condensed phases, particularly since complete ab initio HF (SCRF) geometry optimizations predicted a decrease of the energy gap between 9-AA and 9-AI with an increase in the polarity of the liquid medium (Table 2). Comparison of IR and Raman spectra with theoretical vibrational transitions tend to confirm the existence of amino−imino tautomerism in 9-acridinamine. On the other hand, neither experimental nor theoretical NMR investigations exclude such a phenomenon.

Despite all our efforts, the findings of this work do not enable us to state definitively in which tautomeric form 9-acridinamine exists. This creates the necessity for further investigations on both the tautomeric phenomenon itself and the mechanism of tautomerization. Furthermore, it is important whether derivatives of 9-acridinamine with blocked amino and imino structures can be synthesized and characterized by X-ray analysis (which would confirm the attainability of tautomeric forms) and what their spectral and physicochemical features are as compared with those of the parent compound. These are the problems on which we are currently focusing our attention.

Acknowledgment. The authors thank Dr. P. Sowiński for his help in the NMR studies. The financial support of this work from the Polish State Committee for Scientific Research (KBN) under Grant 2 P303 058 06 (Contract No. PB-0593/P3/94/06) and by the NSF Grant CHE 9116286 is gratefully acknowledged. Our gratifude is extended to The Utah Supercomputing Institute (USI) for the allocation of computer time.

References and Notes

(1) Albert, A. *The Acridines*, 2nd ed.; Edward Arnold Ltd.: London, 1966.

(2) Acheson, R. M. *Acridines*, 2nd ed.; Interscience: New York, 1973.

(3) Kulikov, S. G.; Bykovskaya, L. A.; Samchuk, S. A.; Smirnova, N. P.; Eremenko, A. M. *Zh. Fiz. Khim.* **1991**, *65*, 158.

(4) Rak, J.; Blazejowski, J.; Zauhar, R. J. *J. Org. Chem.* **1992**, *57*, 3720, and references therein.

(5) Mounts, R. D.; Widlund, K.; Gunardi, H.; Perez, J.; Pech, B.; Chambers, J. Q. *J. Electroanal. Chem.* **1992**, *340*, 227.

(6) Smirnova, N. P.; Eremenko, A. M.; Bykovskaya, L. A.; Kulikov, S. G.; Chuiko, A. A. *J. Mol. Struct.* **1992**, *266*, 417.

(7) Lerman, L. S. *J. Mol. Biol.* **1961**, *3*, 18.

(8) Orgel, A.; Brenner, S. *J. Mol. Biol.* **1961**, *3*, 762.

(9) Ferguson, L. R.; Pogai, H.; Turner, P. M. *Mutat. Res.* **1991**, *262*, 227.

(10) Pandey, K. D.; Kashyap, A. K. *Folia Microbiol. (Prague)* **1992**, *37*, 377.

(11) Mattes, W. B.; Kapeghian, J. C.; Lasinski, E. R.; O'Lone, S. D.; Puri, E. C.; Matheson, D. W. *Environ. Mol. Mutagen.* **1993**, *22*, 46.

(12) Tomosaka, H.; Omata, S.; Anzai, K. *Biosci., Biotechnol., Biochem.* **1994**, *58*, 1420.

(13) Kopsidas, G.; Macphee, D. G. *Mutat. Res.* **1994**, *306*, 111.

(14) Kellmann, A. *J. Phys. Chem.* **1977**, *81*, 1195.

(15) Kubota, Y.; Motoda, Y. *J. Phys. Chem.* **1980**, *84*, 2855.

(16) Diverdi, L. A.; Topp, M. R. *J. Phys. Chem.* **1984**, *88*, 3447.

(17) Wirth, M.; Buchardt, O.; Koch, T.; Nielsen, P. E.; Norden, B. *J. Am. Chem. Soc.* **1988**, *110*, 932.

(18) Friedman, R. A.; Shahin, M.; Zuckerbraun, S. *J. Biomol. Struct. Dyn.* **1991**, *8*, 977.

(19) Baba, Y.; Kunihiro, A.; Kagemoto, A. *Thermochim. Acta* **1992**, *202*, 241.

(20) Nuss, M. E.; Marsh, F. J.; Kollman, P. A. *J. Am. Chem. Soc.* **1979**, *101*, 825.

(21) Miller, K. J. *Macromolecules* **1984**, *17*, 1709.

(22) Alekseev, S. I. *Biol. Membr.* **1993**, *10*, 272.

(23) Costa, A. C. S.; Albuquerque, E. X. *J. Pharmacol. Exp. Ther.* **1994**, *268*, 503.

(24) Graslund, A.; Rupprecht, A.; Strom, G. *Photochem. Photobiol.* **1975**, *21*, 153.

(25) Iwamoto, Y.; Yoshioka, H.; Yanagihara, Y. *Chem. Pharm. Bull.* **1987**, *35*, 2478.

(26) Zhang, L.-H.; Jenssen, D. *Carcinogenesis* **1994**, *15*, 2303.

(27) Grzesiak, S.; Otto, H.; Dencher, N. A. *Biophys. J.* **1989**, *55*, 1101.

(28) Proks, P.; Hianik, T.; Kvasnicka, P. *Gen. Physiol. Biophys.* **1992**, *11*, 441.

(29) Kajikawa, H.; Russell, J. B. *Curr. Microbiol.* **1992**, *25*, 327.

(30) Kitada, M.; Horikoshi, K. *J. Bacteriol.* **1992**, *174*, 5936.

(31) Meyer, S.; Phung, N. H. S.; Tremolieres, A.; DeKouchkovsky, Y. *Photosynth. Res.* **1992**, *32*, 95.

(32) Berczi, A. Moller, I. M. *Eur. Biophys. J.* **1993**, *22*, 177.

(33) Sureshkumar, G. K.; Mutharasan, R. *Biotechnol. Bioeng.* **1993**, *41*, 118; **1993**, *42*, 295.

(34) Diaz, R. S.; Monreal, J. *J. Neurochem.* **1994**, *62*, 2022.

(35) Acheson, R. M.; Burstall, M. L.; Jefford C. W.; Sansom, B. F. *J. Chem. Soc.* **1954**, 3742.

(36) Karyakin A. V.; Shablya, A. V. *Dokl. Akad. Nauk SSSR, Ser. Khim.* **1957**, *116*, 969.

(37) Capomacchia, A. C.; Casper, J.; Schulman, S. G. *J. Pharm. Sci.* **1974**, *63*, 1272.

(38) Capomacchia, A. C.; Schulman, S. G. *J. Pharm. Sci.* **1975**, *64*, 1256.

(39) Short, L. N. *J. Chem. Soc.* **1952**, 4584.

(40) Pushkarev, Z. V.; Kokoshko Z. Yu. *Dokl. Akad. Nauk SSSR* **1953**, *93*, 77.

(41) Sukhomlinov, A. K. *Zh. Obshch. Khim.* **1958**, *28*, 1038.

(42) Sheinker, Yu. N.; Pieresleni, E. M. *Dokl. Akad. Nauk. SSSR, Ser. Khim.* **1960**, *131*, 1366.

(43) Kokko, J. P.; Goldstein, J. H. *Spectrochim. Acta* **1963**, *19*, 1119.

(44) Li, F. N.; Rodin, O. G.; Redchenko, V. V.; Traven, V. F. *Zh. Obshch. Khim.* **1991**, *61*, 186.

(45) Rak, J.; Blazejowski, J. *J. Photochem. Photobiol. A* **1992**, *67*, 287.

(46) Hehre, W. J.; Radom, L.; Schleyer, P. v. R.; Pople, J. A. *Ab initio Molecular Orbital Theory*; Wiley: New York, 1986.

(47) *Density Functional Methods in Chemistry*; Labanowski, J. K., Andzelm, J. W., Eds.; Springer Verlag: New York, 1991.

(48) Baker, J. *J. Comput. Chem.* **1986**, *7*, 385; **1988**, *9*, 465.

(49) Schlegel, H. B. In *Modern Electronic Structure Theory: Geometry Optimization on Potential Energy Surfaces*; Schlegel, H. B., Ed.; World Scientific Publishing: Singapore, 1994.

(50) Hariharan, P. C.; Pople, J. A. *Theor. Chim. Acta* **1973**, *28*, 213.

(51) Francl, M. M.; Pietro, W. J.; Hehre, W. J.; Binkley, J. S.; Gordon, M. S.; DeFrees, D. J.; Pople, J. A. *J. Chem. Phys.* **1972**, *77*, 3654.

(52) Becke, A. D. *Phys. Rev. A* **1988**, *38*, 3098.

(53) Becke, A. D. *J. Chem. Phys.* **1993**, *98*, 1372, 5648.

(54) Lee, C.; Yang, W.; Parr, R. G. *Phys. Rev. B* **1988**, *37*, 785.

(55) Rzepa, H. S.; Man, Yin Yi; Karelson, M. M.; Zerner, M. C. *J. Chem. Soc., Perkin Trans. 2* **1991**, 635.

(56) Wong, M. W.; Wiberg, K. B.; Frisch, M. J. *J. Am. Chem. Soc.* **1992**, *114*, 523, 1645.

(57) Foresman, J. B.; Frish, A. *Exploring Chemistry with Electronic Structure Methods: A Guide to Using Gaussian*; Gaussian, Inc.: Pittsburgh, PA, 1993.

(58) Møller, C.; Plesset, M. S. *Phys. Rev.* **1934**, *46*, 618.

(59) Handy, N. C.; Tozer, D. J.; Laming, G. J.; Murray, C. W.; Amos, R. D. *Isr. J. Chem.* **1993**, *33*, 331.

(60) Ditchfield, R. *Mol. Phys.* **1974**, *27*, 789.

(61) Wolinski, K.; Hinton, J. F.; Pulay, P. *J. Am. Chem. Soc.* **1990**, *112*, 8251.

(62) Gauss, J. *J. Chem. Phys.* **1993**, *99*, 3629.

(63) Frisch, M. J.; Trucks, G. W.; Schlegel, H. B.; Gill, P. M. W.; Johnson, B. G.; Wong, M. W.; Foresman, J. B.; Robb, M. A.; Head-Gordon, M.; Replogle, E. S.; Gomperts, R.; Andres, J. L.; Raghavachari, K.; Binkley, J. S.; Gonzales, C.; Martin, R. L.; Fox, D. J.; DeFrees, D. J.; Baker, J.; Stewart J. J. P.; Pople J. A. *Gaussian 92/DFT*, Revision F.2; Gaussian, Inc.: Pittsburgh, PA, 1993.

(64) Frisch, M. J.; Trucks, G. W.; Schlegel, H. B.; Gill, P. M. W.; Johnson, B. G.; Robb, M. A.; Cheeseman, J. R.; Keith, T.; Petersson, G. A.; Montgomery, J. A.; Raghavachari, K.; Al-Laham, M. A.; Zakrzewski, V. G.; Ortiz, J. V.; Foresman, J. B.; Cioslowski, J.; Stefanov, B. B.; Nanayakkara, A.; Challacombe, M.; Peng, C. Y.; Ayala, P. Y.; Chen, W.; Wong, M. W.; Andres, J. L.; Replogle, E. S.; Gomperts, R.; Martin, R. L.; Fox, D. J.; Binkley, J. S.; DeFrees, D. J.; Baker, J.; Stewart J. J. P.; Head-Gordon, M.; Gonzales, C.; Pople J. A. *Gaussian 94*, Revision B.2; Gaussian, Inc.: Pittsburgh, PA, 1995.

(65) Mulliken, R. S. *J. Chem. Phys.* **1955**, *23*, 1833, 1841.

(66) Available from Wavefunction, Inc., 18401 Von Karman, Suite 370, Irvine, CA 92715.

(67) Besler, B. H.; Merz, K. M.; Kollman, P. A. *J. Comput. Chem.* **1990**, *11*, 431.

(68) Atkins, P. W. *Physical Chemistry*, 5th ed.; Oxford University Press: Oxford, 1994.

(69) CODATA recommended key values for thermodynamics: *J. Chem. Thermodyn.* **1978**, *10*, 903.

(70) *Handbook of Chemistry and Physics*, 73 ed.; Lide, D. R., Ed.; CRS Press: Boca Raton, FL, 1992−1993.

(71) Croasman, R.; Carlson, R. M. K. *Two-Dimensional NMR Spectroscopy: Applications for Chemists and Biochemists*, 2nd ed.; VCH Publishers Inc.: New York, 1994.

(72) Chaudhuri, S. *J. Chem. Soc., Chem. Commun.* **1983**, 1242.

(73) Allen, F. H.; Kennard, O.; Watson, D. G.; Brammer, L.; Orpen, A. G.; Taylor, R. *J. Chem. Soc., Perkin Trans. 2* **1987**, S1.

(74) Willis, J. B.; *Trans. Faraday Soc.* **1947**, *43*, 97.

(75) Lubkowski, J.; Janiak, T.; Czerminski, J.; Blazejowski, J. *Thermochim. Acta* **1989**, *155*, 7.

(76) Pople, J. A.; Luke, B. T.; Frisch, M. J.; Binkley, J. S. *J. Phys. Chem.* **1985**, *89*, 2198.

(77) Sana, M.; Leroy, G. *Ann. Soc. Sci. Bruxelles, Ser. 1* **1991**, *105*, 67.

(78) Pedley, J. B.; Naylor, R. D.; Kirby, S. P. *Thermochemical Data of Organic Compounds*, 2nd ed.; Chapman and Hall: London, New York, 1986.

(79) Hehre, W. J.; Ditchfield, R.; Radom, L.; Pople, J. A. *J. Am. Chem. Soc.* **1970**, *92*, 4796.

(80) Shibaev, A. Yu.; Puzanov, Yu. V. *Zh. Fiz. Khim.* **1989**, *63*, 888.

(81) Johnson, B. G.; Gill, P. M. W.; Pople, J. A. *J. Chem. Phys.* **1993**, *98*, 5612.

(82) Dewar, M. J. S.; Ford, G. P. *J. Am. Chem. Soc.* **1979**, *101*, 5558.

(83) Koopmans, T. *Physica* **1934**, *1*, 104.

(84) Trickey, S. B. In *Conceptual Trends in Quantum Chemistry*; Kryachko, E. S., Calais, J. L., Eds.; Kluwer Academic Publishers: Dordrecht, 1994.

(85) Hush, N. S.; Pople, J. A. *Trans. Faraday Soc.* **1955**, *51*, 600.

(86) Roothaan, C. C. J. *Rev. Mod. Phys.* **1951**, *23*, 61.

(87) Warren, D. S.; Gimarc, B. M. *J. Am. Chem. Soc.* **1992**, *114*, 5378.

(88) Hadzi, D.; Koller, J.; Hodoscek, M.; Kocjan, D. In *Modeling of Structure and Properties of Molecules*; Maksic, Z. B., Ed.; Ellis Harwood Ltd.: London, 1987.

(89) Stephens, P. J.; Devlin, F. J.; Chabalowski, C. F.; Frisch, M. J. *J. Phys. Chem.* **1994**, *98*, 11623.

(90) Karyakin, A. V.; Grigorovskii, A. M.; Yaroslavskii, N. G. *Dokl. Akad. Nauk SSSR* **1949**, *67*, 679.

(91) Gurevich, A. I.; Sheinker, Yu. N. *Zh. Fiz. Khim.* **1962**, *36*, 734.

(92) Bacon, N.; Boulton, A. J.; Brownlee, R. T. C.; Katritzky, A. R.; Topsom, R. D. *J. Chem. Soc.*, **1965**, 5230.

(93) Abe, Y.; Nakao, R.; Horii, T.; Kitao, T.; Nakazumi, H.; Matsui, M. *Chem. Funct. Dyes, Proc. Int. Symp., 2nd* **1992** (Pub. 1993), 28.

(94) Kalinowski, H.-O.; Berger, S.; Braun, S. *Carbon-13 NMR Spectroscopy*; Wiley: Chichester, 1991.

(95) Faure, R.; Galy, J. P.; Vincent, E. J.; Elguero, J.; Galy, A. M.; Barbe J. *Chem. Scr.* **1980**, *15*, 62.

(96) Galy, J. P.; Faure, R.; Barbe, J.; Elguero, J. *Spectrosc. Lett.* **1988**, *21*, 809.

(97) Sundquist, W. I.; Bancroft, D. P.; Lippard, S. J. *J. Am. Chem. Soc.* **1990**, *112*, 1590.

(98) Poirier, R. A.; Yu, D.; Surjan, P. R. *Can. J. Chem.* **1991**, *69*, 1589.